

**Performance Analysis of Wheel and Rail Contact  
by Nature of Material Characteristics  
– a Contact Mechanics Approach**

V. C. SATHISH GANDHI

*Department of Mechanical Engineering,  
University College of Engineering Nagercoil,  
Anna University: Tirunelveli Region,  
Konam, Nagercoil – 629004, Tamilnadu, India  
vcsgandhi@gmail.com*

R. KUMARAVELAN

*Department of Mechanical Engineering,  
Velalar College of Engineering and Technology,  
Erode – 638012, Tamilnadu, India*

S. RAMESH

*Department of Mechanical Engineering,  
Annai Mathammal Sheela Engineering College,  
Namakkal – 637013, Tamilnadu, India*

M. THANMANASELVI

*Department of Civil Engineering,  
University College of Engineering  
Nagercoil, Anna University: Tirunelveli Region,  
Konam, Nagercoil – 629004, Tamilnadu, India*

K. SRIRAM

*Faculty Associate, Department of Mechanical Engineering,  
Amrita School of Engineering,  
Coimbatore – 641 112, Tamilnadu, India*

Received (11 April 2014)

Revised (16 September 2014)

Accepted (21 September 2014)

The study aims on by contact analysis of a cylindrical wheel and a rail structure of I-section with considering the material properties of an elastic–plastic adhesive frictional contact. Different materials are considered for the analysis based on Young's modulus and yield strength ratio ( $E/Y$ ). The contact analysis of this model has been carried out using analysis software ANSYS. The simulation results shows that the maximum stress and strain developed at a point near by the contact edge for lower  $E/Y$  value of material and move along the center of a straight line in the contact region between wheel and rail if the  $E/Y$  value increases. The results are compared with the basic contact model and shows that good agreement for the nature of material dependence.

*Keywords:* Contact analysis,  $E/Y$  ratio, stress, strain.

## 1. Introduction

While Classical Mechanics deals solely with bulk material properties Contact Mechanics deals with bulk properties that consider surface and geometrical constraints. The theory of contact mechanics is concerned with the stresses and deformation that arise when the surfaces of two solid bodies are brought into contact. The two surfaces that fit exactly or closely together without deformation are called "conforming contacts", and the surfaces, or one of the two surfaces that deform when there is a contact area in between them are called "non-conforming contacts" [15]. In Mechanical Engineering Design the assignment of structural integrity is a key part. In this paper the basic model of wheel and rail contact is considered the study of material dependency to estimate the contact stress and strain to evaluate the wear rate based on the material dependency. The computer based model has been developed for different materials and the models are studied.

## 2. Theoretical background

The contact condition between the wheel and rail contact, the contact zone surfaces and bulk material must be strong to resist the heavy loads and dynamic response. The contact zone must be small compared with the overall dimensions and its shape of the wheel and rail. The contact zone size and shape in the wheel and rail contact has been estimated from the Hertz theory of elliptical contact with the following assumptions: the material is linear elastic, the smooth contact surfaces, the surfaces are described by second degree and no friction between the contact surfaces. Liu [1] studied stresses due to tangential and normal loads on an elastic solid with application to some contact stress problems. Haines and Ollerton investigated contact stress distribution on elliptical contact surfaces subjected to radial and tangential forces [2]. Some useful results in the classical Hertz contact problem were presented by Sackfield and Hills [3]. The wheel-rail contact problem can be formulated as a rolling contact problem between two nonlinear profiles in the presence of friction. In the present study the behaviour of nonlinear profile by considering the material properties was carried out.

## 3. Literature review

Contact analysis can be traced back to 1882, in which Hertz studied the elastic contact between two glass lenses. The Hertz theory is restricted to the normal frictionless contact between an elastic half-space with small deformation. Vahid Monfared [4] presented the contact stress analysis in rolling bodies by finite element method to analyse the pressure of collection of the wheel and rail, elliptical, rectangular and circular contact surfaces are assumed for this study using classical mechanics approach. Jabbar-Ali Zakeri et al [5] studied the effect of geometrical parameters on the behaviour of dynamic interaction of wheel-rail is being investigated through a parametric study. Zong et al [6] analyzed a three-dimensional wheel-rail contact model in the finite element framework is used for the analysis of the rail ends under wheel contact loading. J. J. Zhu et al [7] studied an adaptive wheel-rail contact model with radial spring is developed for prediction of wheel-rail normal contact force. Mehmet Ali Arslan and Oguz Kayabasi [8] has presented the fundamental way of handling Rail-Wheel contact problems from the FEA

standpoint, and highlighted the required steps for more realistic 3D solutions to these types of problems. Pramod Murali Mohan [9] has studied the applications of railway wheel viz., the behaviour of wheel subjected to thermal and structural loading and the combined loading. He pointed out that an excessive braking of wheel leads to thermal overloading which results in fatigue, crack propagation leading to fracture and wear. Santamaria et al [10] presented a wear index prediction for wheel-rail contact model of multiple contact patches for the two contact point situation using three-dimensional analysis of surfaces including the influence of the angle of attack. In these cases the front wheel set's angle of attack tends to adopt high values that have a considerable effect on the localisation of contact patches, increasing creep and wear indices. Braghin et al [11] proposed a mathematical model to predict a railway wheel profile evaluation due to wear. Donzella and Petrogalli [12] proposed a failure assessment diagram for the evaluation of the safe working area of components subjected to rolling contact loading. The rolling contact fatigue limitation in terms of non-propagation condition of inherent defects. Static fracture and ratchetting limitations are also added to the diagram. Vahid Monfared [13] has proposed a new formulation of contact stress for two rolling bodies is presented, and its results are close to the hertz stress formulation. The analysis of stress, fracture, prediction of fracture and path of crack motion in rail and wheel are studied statically. Monfared and Khalili [14] presented the mechanical behaviour of the one Lead-Zirconate-Titanate by its atomic number and its certain mechanical behaviour is simulated by the mathematical modeling and ABAQUS software for smart materials, as well as prediction of mechanical behaviors. The detail reviewed of wheel and rail contact analysis pointed out the wear calculation, failure analysis and so on. The material dependency analysis are not pointed out in the literature review.

#### 4. Materials and methods

The present three-dimensional analysis aims to study the contact stress and strain for different E/Y values of material, under the loading condition of the wheel and rail contact model. The finite element analysis software "ANSYS" has been used to carry out this analysis, in an axisymmetric condition. Hence, a quarter wheel (cylinder) is considered for the analysis. The 3D finite element contact model of a wheel and rail is shown in Fig. 1.

For this contact model the contact pair is created and confirmed between the wheel and rail as shown in Fig. 2. The dimensions of the model are as follows: diameter of the wheel is 10 mm and wheel thickness is 20 mm. Rail dimensions: base width is 40 mm; head width is 20 mm; head thickness is 5 mm; and rail height is 20 mm. For this investigation both wheel and rail are discretized by eight-noded brick 185 element. The upper surface of rail is selected as target surface (target 169) and curved surface of wheel is selected as contact surface (conta 172). The nodes lying on the axis of the wheel and rail are restricted to move in the radial direction. Also the nodes in the bottom of the rail are fixed in all the directions. The constrained and meshed model is shown in Fig. 4. The average wheel size used for this analysis is 5 mm radius.

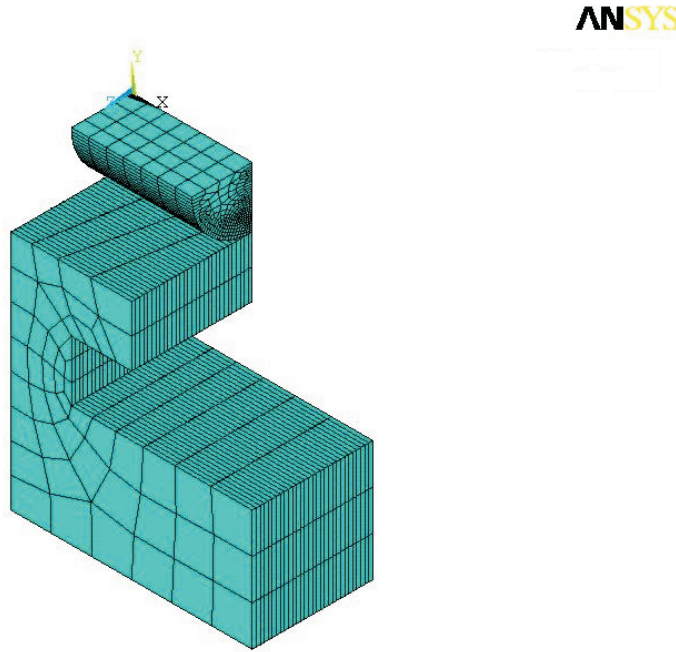


**Figure 1** Finite element contact model of a wheel and rail (3D)

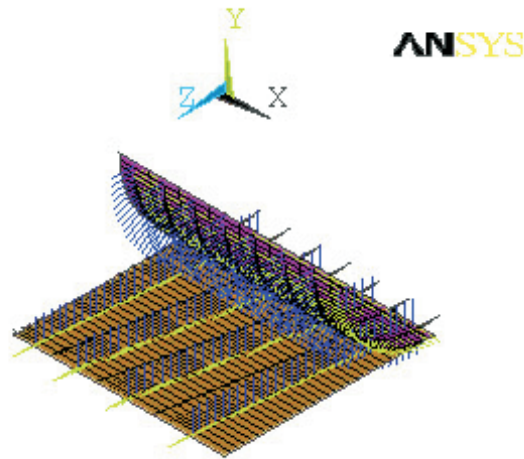
The material properties are selected based on the Young's modulus to yield strength ratio [16]. Poisson's ratio = 0.32 and the friction coefficient at the interface between wheel and the rail is 0.1. The load is applied as a constant pressure of 0.5 MPa on the top surface of the wheel. The different Young's modulus to yield strength ratio is considered for analysis between 100 and 700. The E/Y ratio is considered for this analysis is less than 1000 for high yield strength of the material.

## **5. Finite Element simulation of a wheel and rail contact**

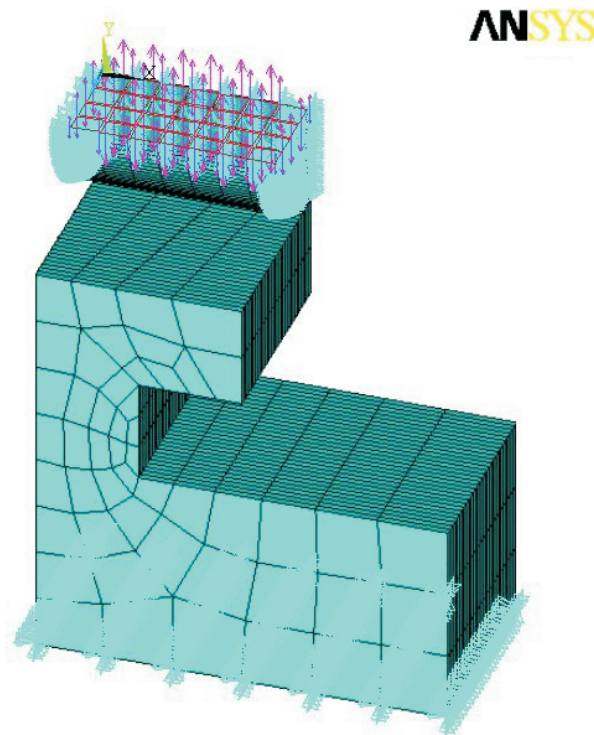
The finite element simulation has been performed for different E/Y values of material such as 150, 296.6, 363.6, 470, 540, 660. The performance study has been carried out for these materials based on contact stress and strain with considering friction.

### **5.1. Analysis of stress distribution for different materials**

The analysis is performed for different materials having E/Y value between 100 and 700. The load is applied in the top surface of the wheel in terms of constant pressure of 0.5 MPa. Initially the contact is of a point contact, then it is a line contact after



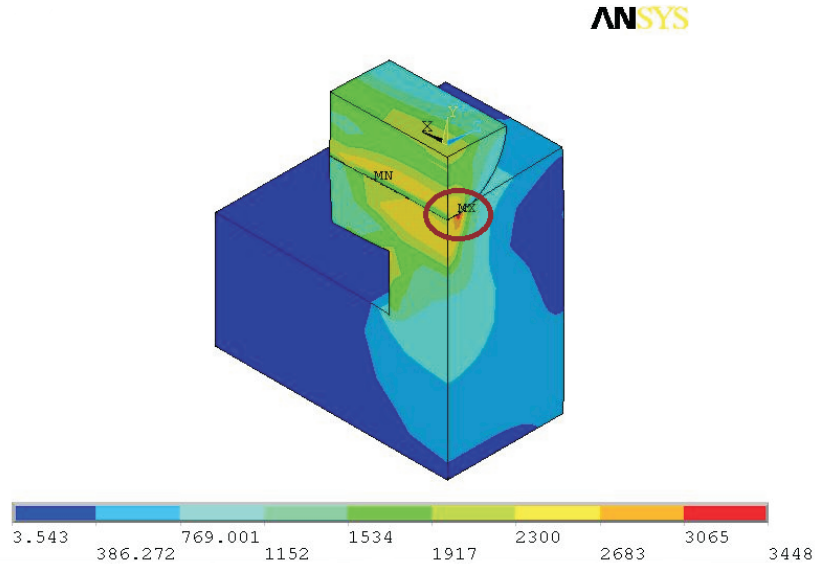
**Figure 2** Plot for Contact pair creation



**Figure 3** Meshed and constrained model

load is applied. The distribution of stress has been estimated between the wheel and rail. The stress distribution plots are given for the minimum and maximum values of  $E/Y$  ratios.

Fig. 4 shows the stress distribution for the material ( $E/Y = 150$ ) for wheel and rail contact model. The maximum stress of  $3448 \text{ N/mm}^2$  is developed at the edge of the contact area for this material. The maximum stress area is enclosed in a circle as shown in Fig. 4. It is observed that for low  $E/Y$  value of material the maximum stress is developed at the edge of the contact.



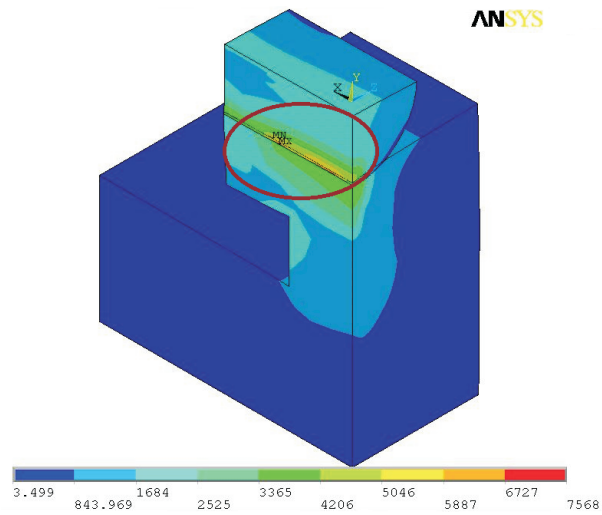
**Figure 4** Plot for Stress Distribution for the material  $E/Y = 150$

Fig. 5 shows the stress distribution for the material ( $E/Y = 660$ ) for wheel and rail contact model. The maximum stress of  $7568 \text{ N/mm}^2$  is developed at the center of the line of contact for this material. The maximum stress area is enclosed in a circle as shown in Fig. 5. It is observed that for high  $E/Y$  value of material the maximum stress is developed at the center of the line of contact.

## 5.2. Analysis of strain distribution for different materials

The strain analysis has been carried out for the wheel and rail contact model for different materials. The strain distribution plots are given for the minimum and maximum values of  $E/Y$  ratios.

Fig. 6 shows the strain distribution for the material ( $E/Y = 150$ ) for wheel and rail contact model. The maximum strain of  $0.051094$  is developed at the edge of the contact for this material. The maximum strain area is enclosed in a circle as shown in Fig. 6.



**Figure 5** Plot for Stress Distribution for the material  $E/Y = 660$

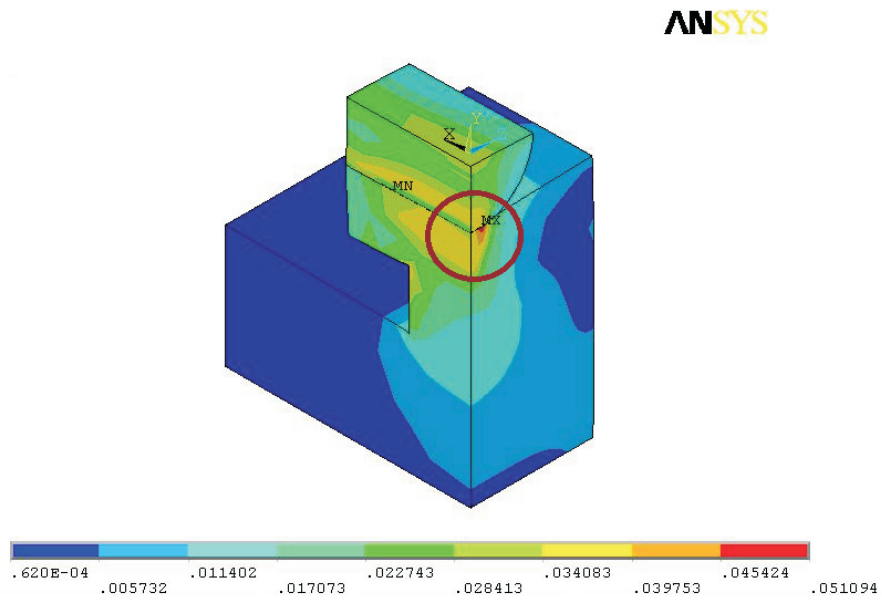


**Figure 6** Plot for Strain Distribution for the material  $E/Y = 150$

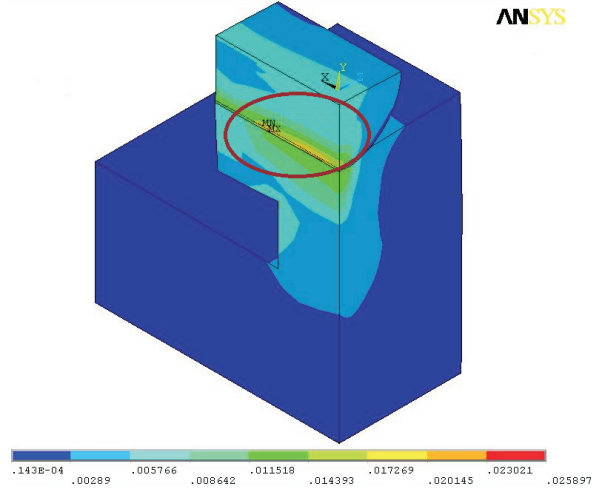


**Figure 7** Plot for Strain Distribution for the material  $E/Y = 660$

Fig. 7 shows the strain distribution for the material ( $E/Y = 660$ ) for wheel and rail contact model. The maximum strain of 0.025897 is developed at the center of line of contact for this material. The maximum strain area is enclosed in a circle as shown in Fig. 7. It is observed that for the low  $E/Y$  of material the maximum strain is developed at the edge of the contact and for high  $E/Y$  value of material the maximum strain is migrated into the center of the line of contact between the wheel and rail.

### 5.3. Analytical study of contact model for different materials

The analytical study has been done for the model proposed by Jackson and Green (JG – model) [17]. The main objective of this study is to find out the material distinguishing of elastic-plastic model in the contact analysis based on the various parameters like, yield strength, hardness and dimensionless interference. JG – model proposed the empirical relation of hardness to yield strength ratio is given by:

$$\frac{H_G}{Y} = 2.84 \left[ 1 - \exp \left( -0.82 \left( \frac{\pi CY}{2E'} \sqrt{\omega^*} \left( \frac{\omega^*}{\omega_t^*} \right)^{B/2} \right)^{-0.7} \right) \right] \quad (1)$$

$$\omega_c = \left( \frac{\pi CS_y}{2E'} \right) R \quad (2)$$

$$C = 1.295 \exp(0.736v) \quad (3)$$

where:

$$\omega_t^* = 1.9 \quad v = 0.32 \text{ and } H_G = \text{Hardness (H)}$$

$$B = 0.14 \exp(23Y/E) \quad (4)$$



## 6. Results and Discussion

The wheel and rail contact simulation has been performed for different materials using the analysis software 'Ansys'. The results were obtained from the simulations and analytical study are discussed as follows:

The stress distribution in this contact model has been performed for different E/Y values. Tab. 1 shows the stress distribution values for different E/Y values of materials.

**Table 1** Stress distribution values for different E/Y values

| S.No. | E/Y values of material | Stress distribution (FEA) N/mm <sup>2</sup> |
|-------|------------------------|---|
| 1     | 150                    | 3448  |
| 2     | 296.6                  | 3880  |
| 3     | 363.6                  | 3722  |
| 4     | 470                    | 3886  |
| 5     | 540                    | 4033  |
| 6     | 660                    | 7568  |

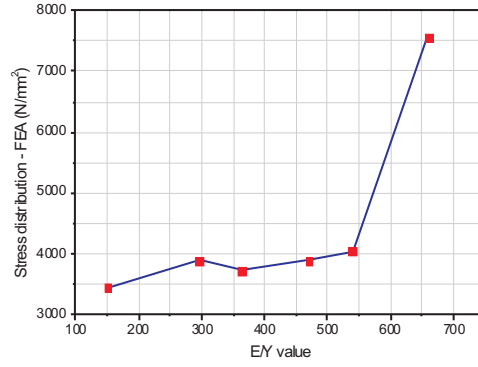
The strain distribution in this contact model has been performed for different E/Y values. Tab. 2 shows the strain distribution values for different E/Y values of materials.

**Table 2** Strain distribution values for different E/Y values

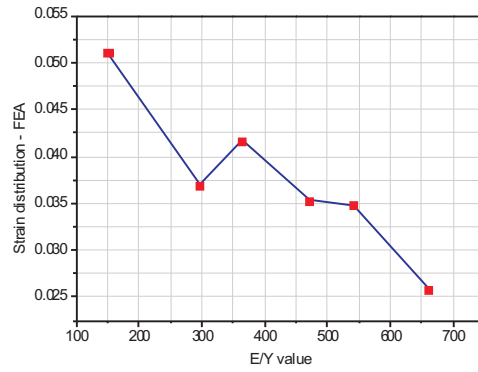
| S.No. | E/Y values of material | Strain distribution (FEA) |
|-------|------------------------|---------------------------|
| 1     | 150                    | 0.051094                  |
| 2     | 296.6                  | 0.03698                   |
| 3     | 363.6                  | 0.041733                  |
| 4     | 470                    | 0.03528                   |
| 5     | 540                    | 0.034863                  |
| 6     | 660                    | 0.025879                  |

Fig. 8 shows the relationship between stress distribution and E/Y values of different material for wheel and rail contact model. The stress value increases and again decreases after that increases for further increases in E/Y values. It shown that the critical value of E/Y value between 296.6 and 363.6.

Fig. 9 shows the relationship between strain distribution and E/Y values of different material for wheel and rail contact model. The strain value increases and again decreases after that increases for further increases in E/Y values. It shown that the critical value of E/Y value between 296.6 and 363.6.



**Figure 8** Stress distribution Vs E/Y value



**Figure 9** Strain distribution Vs E/Y value

Fig. 10 shows the relationship between stress, strain distribution and E/Y values of different material for wheel and rail contact model. It is shown that the stress is not directly propositional to the strain it is inversely proportional to each other. This will be happened if the material beyond the elastic limit. At the inception of the elastic-plastic region the elastic regime has more dominated than the plastic. At the end of the elastic-plastic region the plastic has more dominated than elastic. In this wheel and rail contact analysis, the analysis has been performed in the elastic-plastic region.

The hardness to yield strength ratio is calculated from Equation 1 for the various E/Y values and dimensionless interference up to 90. The Hardness to Yield strength ratio (H/Y) values are shown in the Tab. 3.

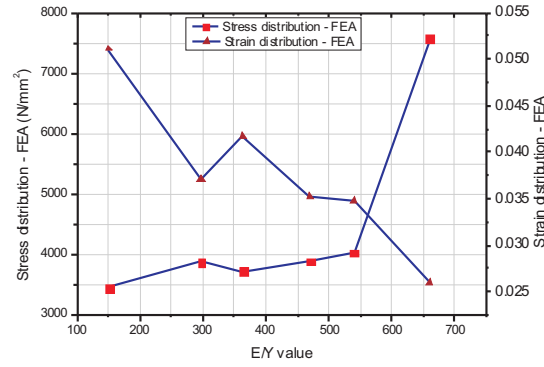


**Figure 10** Stress and strain distribution Vs E/Y value

**Table 3** Hardness to yield strength ratio (H/Y) for different E/Y values

| S. No. | Dimensionless interference<br>$\omega/\omega_c=\omega^*$ | Hardness to yield strength ratio (H/Y) |       |        |       |        |       |
|--------|--|--|-------|--------|-------|--------|-------|
|        |  | E/Y value                              |       |        |       |        |       |
|        |  | 150                                    | 296.6 | 363.6  | 470   | 540    | 660   |
| 1      | 10   | 2.8306                                 | 2.839 | 2.8399 | 2.84  | 2.84   | 2.84  |
| 2      | 20   | 2.801                                  | 2.837 | 2.8392 | 2.84  | 2.84   | 2.84  |
| 3      | 30   | 2.7665                                 | 2.833 | 2.8373 | 2.839 | 2.8397 | 2.84  |
| 4      | 40   | 2.729                                  | 2.826 | 2.8343 | 2.838 | 2.8393 | 2.84  |
| 5      | 50   | 2.694                                  | 2.818 | 2.8303 | 2.836 | 2.8386 | 2.839 |
| 6      | 60   | 2.659                                  | 2.809 | 2.8255 | 2.834 | 2.8377 | 2.839 |
| 7      | 70   | 2.626                                  | 2.8   | 2.82   | 2.832 | 2.8365 | 2.838 |
| 8      | 80   | 2.595                                  | 2.79  | 2.814  | 2.829 | 2.835  | 2.837 |
| 9      | 90   | 2.565                                  | 2.78  | 2.808  | 2.827 | 2.8334 | 2.837 |

From the Tab. 3 it is observed that the value of hardness to yield strength ratio is equal to 2.8 for all the E/Y values except 150 and 296.6.

Fig. 11 shows the relationship between the hardness to yield strength ratio and dimensionless interference for different E/Y values. From this graph it is observed that the interference value increases the hardness to yield strength decreases. For the E/Y values 150 and 296.6 this ratio never reaches 2.8 upto the dimensionless interference 90 compared with the rest of E/Y values. It shows that the Young's modulus to yield strength ratio is very important for the contact analysis models. From this study results it is observed that in the elastic-plastic region the material upto  $E/Y = 296.6$  is dependent on the material characteristic and rest of E/Y values it is independent of material characteristics in the contact analysis. So the critical value of E/Y is identified between 296.6 and 363.6.

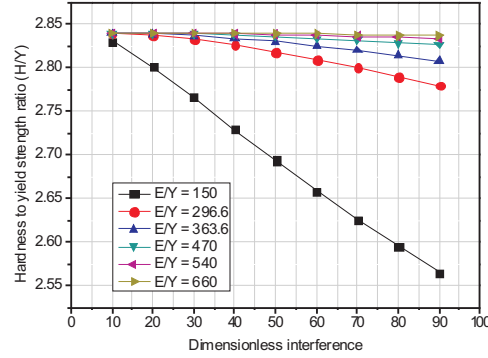


**Figure 11** Hardness to yield strength ratio ( $H/Y$ ) Vs  $E/Y$  value

## 7. Conclusion

The performance for wheel and rail contact has been studied for different  $E/Y$  values of material in the elastic-plastic region. The studies carried out on both simulation and analytical basic model. The simulation results of wheel and rail contact model shows that the maximum stress and strain are occurred in the edge of the contact for low  $E/Y$  value of material and migrated to the center point of the line of contact between the wheel and rail for high  $E/Y$  value of material. It shows that the contact analysis is not completely independent of material characteristics in the elastic-plastic region. To verify the simulation results the analytical study has been carried out for the basic model proposed for flat and sphere contact analysis. This results shows that the hardness to yield strength ratio is equal to 2.8 for the material  $E/Y$  greater than 296.6. For low  $E/Y$  value less than 296.6 this ratio is not equal to 2.8. Hence in the contact analysis between the rigid and deformable bodies are depended on the material characteristic in the elastic-plastic region. The critical value of  $E/Y$  has been identified as between 296.6 and 363.6.

## References

- [1] **Smith, J. O. and Liu, C. K.:** Stresses due to tangential and normal loads on an elastic solid with application to some contact stress problem, *J. Appl. Mech.*, 20, 157–166, **1953**.
- [2] **Haines, D. J. and Ollerton, E.:** Contact stress distribution on elliptical contact surfaces subjected to radial and tangential forces, *Proc. of Inst. of Mechanical Engineers*, London, 177(4), 45–54, **1963**.
- [3] **Sackfield, A. and Hills, D. A.:** Some useful results in the classical Hertz contact problem, *Journal of Strain Analysis*, London, 18(2), 101–105, **1983**.
- [4] **Vahid Monfared:** Contact Stress Analysis in Rolling Bodies by Finite Element Method (FEM) Statically, *Journal of Mechanical Engineering and Automation*, 2(2), 12–16, **2012**.

- [5] **Jabbar–Ali Zakeri, Masoud Fathali and Nima Boloukian Roudsari:** Effects of Rail Cant on Wheel–Rail Contact Forces in Slab Tracks, *International Journal of Mechanics and Applications*, 1(1), 12–21, **2011**.
- [6] **Zong, N. and Dhanasekar, M.:** Analysis of Rail Ends under Wheel Contact Loading, *International Journal of Aerospace and Mechanical Engineering*, 6, 452–460, **2012**.
- [7] **Zhu, J. J., Ahmed, A. K. W. and Rakheja, S.:** An Adaptive Contact Model for simulation of Wheel–rail Impact Load due to a Wheel Flat, *13<sup>th</sup> National Conference on Mechanisms and Machines*, IISc, Bangalore, India, 12–13, **2007**.
- [8] **Mehmet Ali Arslan and Oguz Kayabasi:** 3–D Rail–Wheel contact analysis using FEA, *Advances in Engineering Software*, 45, 325–331, **2012**.
- [9] **Pramod Murali Mohan:** Analysis of Railway Wheel to study Thermal and Structural Behaviour, *International Journal of Scientific & Engineering Research*, 3(11), **2012**.
- [10] **Santamaria, J., Vadillo, E. G. and Oyarzabal, O.:** Wheel–rail wear index prediction considering multiple contact patches, *Wear*, 267, 1100–1104, **2009**.
- [11] **Braghin, F., Lewis, R., Dwyer–Joyce, R. S. and Bruni, S.:** A mathematical model to predict railway wheel profile evolution due to wear, *Wear*, 261, 1253–1264, **2006**.
- [12] **Donzella, G. and Petrogalli, C.:** A failure Assessment Diagram for Components Subjected to Rolling Contact Loading, *International Journal of Fatigue*, 32(2), 256–268, **2010**.
- [13] **Vahid Monfared:** A new analytical formulation for contact stress and prediction of crack propagation path in rolling bodies and comparing with finite element model (FEM) results statically, *International Journal of the Physical Sciences*, 6(15), 3589–3594, **2011**.
- [14] **Monfared, V. and Khalili, M. R.:** Investigation of Relations between Atomic Number and Composition Weight Ratio in PZT and SMA and Prediction of Mechanical Behavior, *Acta Phys. Pol. A.*, 120, 424–428, **2011**.
- [15] **Johnson, K. L.:** Contact Mechanics, *Cambridge University Press*, Cambridge, **1985**.
- [16] **Davis, J. R.:** Metals Handbook, 2<sup>nd</sup> ed., *ASM International: Metals Park*, OH, **1999**.
- [17] **Jackson, R. L. and Green, I.:** A finite element study of elasto plastic hemispherical contact against a rigid flat, *ASME. J. Tribol.*, 127, 343–54, **2005**.

**Nomenclature:**

H or  $H_G$  – hardness

Y – yield strength N/mm<sup>2</sup>

$E'$  – equivalent Young's modulus N/mm<sup>2</sup>

$\nu$  – Poisson's ratio

R – radius of the sphere mm

$\omega^*$  – dimensionless interference

$\omega$  – interference mm

$\omega_c$  – critical interference mm

E – Young's modulus N/mm<sup>2</sup>

E/Y – Young's modulus to Yield strength ratio

B – material constant

C – critical yield stress coefficient

$\omega_t^*$  – interference transitional value from elastic to elasto-plastic behaviour